ISSN 1476-1580

North West Geography

Volume 19, Number 2, 2019

Toward a protocol for UAV surveying in Environmental Sciences

Rory Scott and Neil Entwistle
School of Science, Engineering and Environment, Salford.
n.s.entwistle@salford.ac.uk

Abstract

The use of small unmanned aerial vehicles (sUAV) has significantly enriched surveying in the environmental sciences within the last few years, due partly in technological advances in onboard GPS and more predominantly with associated ease of post-processing using photogrammetric software such as structure from motion. In addition, the use of sUAV photography to generate 3D elevation models of objects and landscapes at high resolutions has proved an easily accessible alternative to often expensive, cumbersome laser scanning systems. Survey spatial coverage can be increased simply through an increase in flight altitude, although resolution is sacrificed, however finding a balance between these two factors is key to producing high quality data, quickly, yet to date a protocol for deployment of UAVs to establish optimal spatial coverage, flight height to resolution ratio, and ground control point spacing, remains missing in the literature. Here, we establish a simple, repeatable methodology, to provide users with knowledge of how to optimize flight plans according to their requirements for resolution and coverage and best practice processing options are detailed to for the generation of orthomosaics and 3D digital elevation models at a variety of resolutions.

Keywords

UAV, Photogrammetry, 3D-Model, Coverage, Resolution, SfM

Introduction and Justification of Study

The affordability and extensive choice of unmanned aerial platforms along with improvements in on-board systems have allowed for a recent exponential growth of their use within academic and industrial areas. The results have been applicable to a multiplicity of scientific fields, from volcanic surveys (e.g. Tobita *et al.*, 2014), riverine research (e.g. Woodget *et al.*, 2016; Entwistle *et al.*, 2019) and studies of vegetation (e.g. Mathews and Jensen, 2013; Moudrý *et al.*, 2019). Among the most powerful applications of UAV photography is the ability to rapidly generate digital elevation models and high resolution orthomosaics of large scale subjects (Siebert and Teizer, 2014). This process is however limited by the conventional restraints of coverage and resolution, which are so often present in nearly every form of remote sensing and data collection system. Whilst literature exists regarding the applicability of UAV field deployment, there is yet to be a study that defines and examines the relationship between spatial coverage and image resolution when surveying in the field. This is often a critical element for researchers or industry to both understand this relationship and ensure the level of detail in the results. In addition, the protocol presented here provides information on how to best plan and manage flights. Fundamentally, this protocol will allow surveyors to work more efficiently and produce quality results within their personal constraints.

Field Background

Most of the early development of earth observation systems took place during the cold war, driven by the intelligence-based nature of the period and correspondingly generous funding from the superpowers. The U-2 high altitude imaging aircraft was perhaps the premier platform of the time, in terms of its imagery coverage and resolving power (Goetz *et al.*, 1985). Vulnerabilities in the system however led to the need for the development of a space-borne platform, resulting in the CORONA satellite programme (Perry, 2012). With global coverage and at resolutions thought unachievable for the era, the capabilities of the platform far exceeded even the expectations of its designers. Despite the undesirable conditions under which such imaging platforms were conceived, these technologies soon found application in peacetime research and laid the groundwork for a new generation of remote sensing systems. The U-2 aircraft platform continues to see service under NASA for

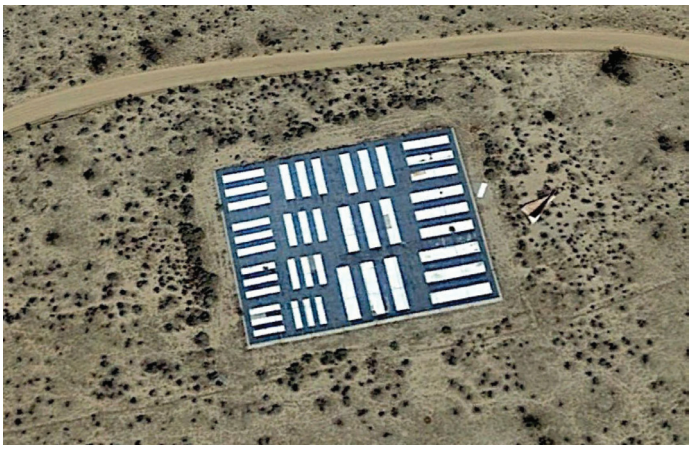

Figure 1: GRT at Edwards AFB, USA. Such targets were used for testing of high-altitude reconnaissance systems. (Image © Google Earth 2019).

metrological research, (Goldhagen *et al.*, 2003, Scott *et al.*, 1990). CORONA satellites also saw non-military, albeit CIA led, application (McDonald, 1995).

As earth observation technologies developed, a means for testing the resolving power and quantifying the spatial resolution of imaging systems was pioneered by the United States Air Force (USAF), where they established a standardised measure of spatial resolution, ground resolved distance (GRD), referring to the dimensions of the smallest distinguishable objects in the image. Their 1951 standard remains in use today and is shown in Figure 1.

GRD was calculated by acquiring another value using Ground Resolution Targets (GRTs) Line pairs per millimetre (LPM). This can then be applied to equation 1:

$$GRD = \frac{H}{(f)(R)} \qquad \textit{Equation 1}$$

where H is altitude, f is camera focal length, and R is LPM, in order to infer spatial resolution. Having seen much of its development in the monochrome film era of photography, the method found film types with a higher contrast ratio (i.e. darker blacks and lighter whites) could deliver notably higher resolutions.

The significant recent use of unmanned aerial platforms within a research capacity has been supplemented by developments in camera sensors and mounting systems, as well as computing and post-processing power (Turner *et al.*, 2012). According to UAV Global's listings, there are 241 standalone commercial UAV manufacturers, as of May 2016 ("Commercial UAV Manufacturers", 2016), with an estimated worth of $10 billion and a projected 20% growth in the civilian sector by 2024. The use of UAVs as a field of remote sensing and environmental science has found them to outperform platforms such as LiDAR, especially in terms of cost and ease of deployment (Hodgson *et al.*, 2013). This paper will inform practitioners seeking to optimise the data collection process for UAV derived 3D DEM generation, allowing for the acquisition of highest quality imagery in the most efficient time period.

Methodology Construction

Role of Field of View and Ground Sampling Distance.

Among other parameters, image resolution is perhaps the most important factor when it comes to overall quality of the texture of generated DEMs and level of detail in orthophotos (Nex & Remondino, 2013). Ground details are often more easily resolved at higher resolutions, by imaging at lower altitudes. Doing so however limits the ground footprint coverage (GFC) for each image and as such, requires more individual images to be captured during the survey, necessitating increased flight times, battery usage, data storage and processing time. Whilst higher resolutions are more desirable if small landscape details are of interest, they are not always feasible for surveys of large extent (where coverage is the more favoured factor). Here, we utilize a proxy for resolution in our methodology: ground sample distance (GSD). This parameter represents the real-world scale of one pixel or the distance between the centres of two pixels i.e. the size of the smallest feature that the user wishes to detect in their survey. For example, for an image with a GSD of 5cm, one pixel would represent 5cm on the ground. Simply flying for the highest possible resolution, (smallest possible GSD) is not always feasible, even if users are not limited by processing time constraints or computing processing power. For generation of the highest quality, blur free orthophotos, image calibration and alignment error must be reduced through employment of ground control points (GCPs). To utilize GCPs effectively however, they must be present in numerous overlapping images. Placing and recording the position of GCPs using high accuracy GPS can be the most laborious part of executing a UAV survey, particularly in the field of environmental science where difficult conditions may compromise workers' ability to access ideal GCP placement or compromise the durability/ survivability of the UAV. By flying with absolute favour for resolution, resulting image GFC can be so narrow that the number of GCPs that would need to be placed, recorded and recollected during the course of the survey would be unfeasibly high, thus why it should always be taken into account, especially for surveys of wide coverage. Image

overlap is also particularly important when generating DEMs using SfM processing methods, specifically when generating 3D point clouds (Neitzel & Klonowski, 2012). SfM software commonly identifies three-dimensional structures by recognising common points in multiple images (Micheletti et al. 2015). The more images in which a specific point in the surveyed environment is documented, the more accurate the resulting point clouds and DEMs will be (Fonstad *et al.*, 2013).

The role of data quantity management and storage capacity also become apparent in such situations. For subjects of particularly wide extent, thousands of images may be captured per flight. This has implications for surveyors using SfM tools to generate DEMs as well as those using only orthophotos. Whilst modern data storage is relatively inexpensive and accessible for those working in developed areas, workers who might be operating in remote field conditions with limited resources for prolonged periods should carefully consider their data capacity and processing capabilities. Users must consider limiting their survey resolution in such situations in order to increase coverage and reduce processing times. As part of the protocol proposed by this paper, we present equations that allow users to calculate an optimal surveying altitude for a GSD or GFC of their choice. Using simple camera parameters, the methodology is universally applicable to nearly any imaging platform:

$$H = \frac{Fl \times GFCw}{Sw} \qquad \textit{Equation 2}$$

where: H is distance to subject (altitude) in meters, Fl is camera focal length in millimetres, Sw is camera sensor width in millimetres, GFCw is the width of the image's ground footprint in meters, GSD is image ground sampling distance in meters and Iw is Image width in pixels.

$$H = \frac{Fl \times GSD}{Sw \times Iw} \qquad \textit{Equation 3}$$

Equation Operation

Equations 2 and 3 operate on the proportional nature of angular and distant parameters inside the camera and in the imaged environment. This allows for trigonometrical calculation of the parameters of one, assuming those of the other are known. Figure 2 illustrates the identifiable angles and distances, which are used to calculate appropriate flying height and image field of view. The upper portion of the diagram shows a highly simplified camera (existing as only a lens and sensor), whilst the lower part illustrates the field of view for the camera. Values for sensor width (Sw) and focal length (Fl) are usually available within manual documentation or image metadata. It should be noted that Equations 2 and 3 use data for width of GFC and camera sensor (in the X-axis), and operate in one dimension, thus width is easily substitutable for height of GFC area and sensor (in the Y-axis).

Ultimately, GFC and GSD dictate the overall quality of resultant outputs and processing time required to obtain them. Rearranging Equations 2 and 3 can be particularly helpful for users whose survey altitudes are restricted but wish to calculate image coverage or GSD in order to identify whether their survey is feasible or not. GSD or GFC can also be calculated as a product of one or the other through use of the width or height of the image in pixels, depending on which dimension (X or Y) was initially selected, as shown in Equations 4 and 5:

$$GSD = \frac{GFCw}{Iw} \qquad \textit{Equation 4}$$

$$GFCw = GSD \times Iw \qquad \textit{Equation 5}$$

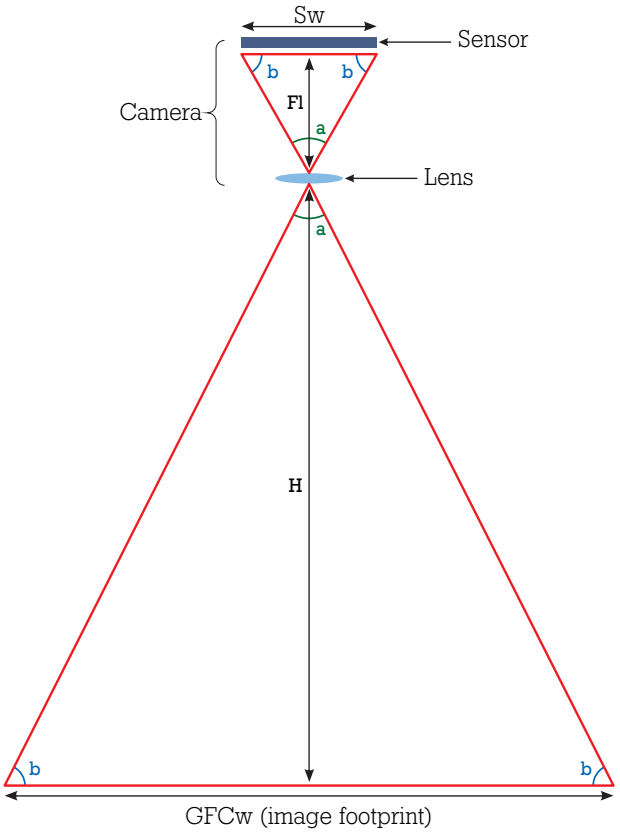

Figure 2: Diagram to illustrate proportionality of angular and distant parameters within a camera and subject environment.

Validation

Workflow development and error estimation is possible by working in reverse with Equation 2 or 3 to calculate known, fixed parameters such as focal length, sensor width or image width, whose values can be found from manual documentation and image metadata. Equations 2 and 3 were tested via reverse calculation using data collected during experiment flight with a DJI Phantom 3 Professional UAV. The drone was ascended to a height of 120m over a fixed point, capturing nadir images at intervals of 5m. A tape measure laid to a length of 20m positioned directly below the UAV allowed for gauging of scale and thus calculation of GFC width for 18 images. Use of Equation 3 then permitted calculation of GSD for each image using the image width in pixels (4000). The inferred measurements of footprint width in all captured images are shown plotted against their respective capture altitude in Figure 3. Calculated values for GSD are also plotted on the secondary axis of Figure 3. Focal length and image width (4mm and 4000 pixels respectively for out Phantom 3) were reverse calculated using Equations 2 and 3, returning values with ±0.3% deviation. Such error may be attributed to the ±0.1m accuracy reading in the live UAV altimeter and marginal error when measuring image GFC, however extracted UAV image metadata will reduce these errors.

Workflow

Flight Planning

Whilst no methodology is universally applicable to all UAV surveys due to the differing natures of and problems presented by environments of interest and imaging subjects, the equations outlined above can however offer a degree of transferability regarding planning for possible survey altitudes. As the primary control upon the variables of image ground coverage and GSD, survey altitude may be considered the most immediately favourable factor to be known when flight planning. It may however be favourable to calculate GFC, GSD or even focal length as the primary control for a survey, especially in situations where one or more parameters may be constrained (altitude being the most common). In such circumstances, the above equations remain capable of providing valuable information. If altitude is restricted, tuning of GFC and GSD is still possible through adjustment camera focal length, calculable via rearrangement of Equations 2 and 3. Similarly, if users wish to restrict survey GSD in order to save data capacity and improve image overlap, or constrain coverage in order to maximise orthophoto and DEM detail, suitable employment of the above equations can facilitate bespoke flight planning and information feedback.

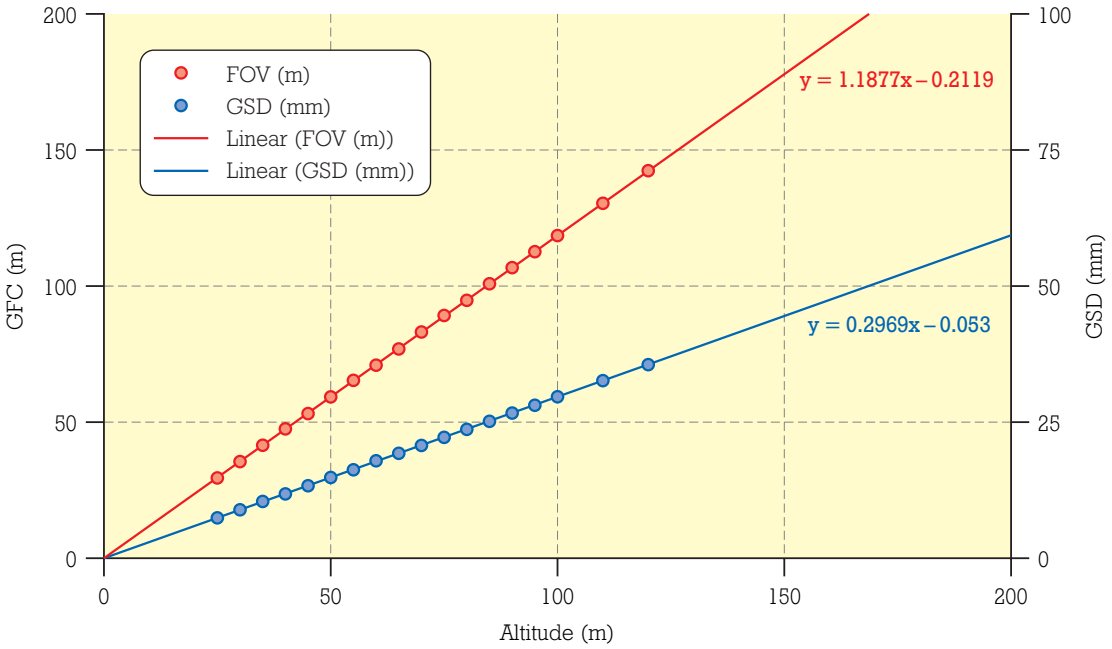

Figure 3: Scatterplot for field of view width and ground sampling distance against altitude with linear trend lines accompanying equations.

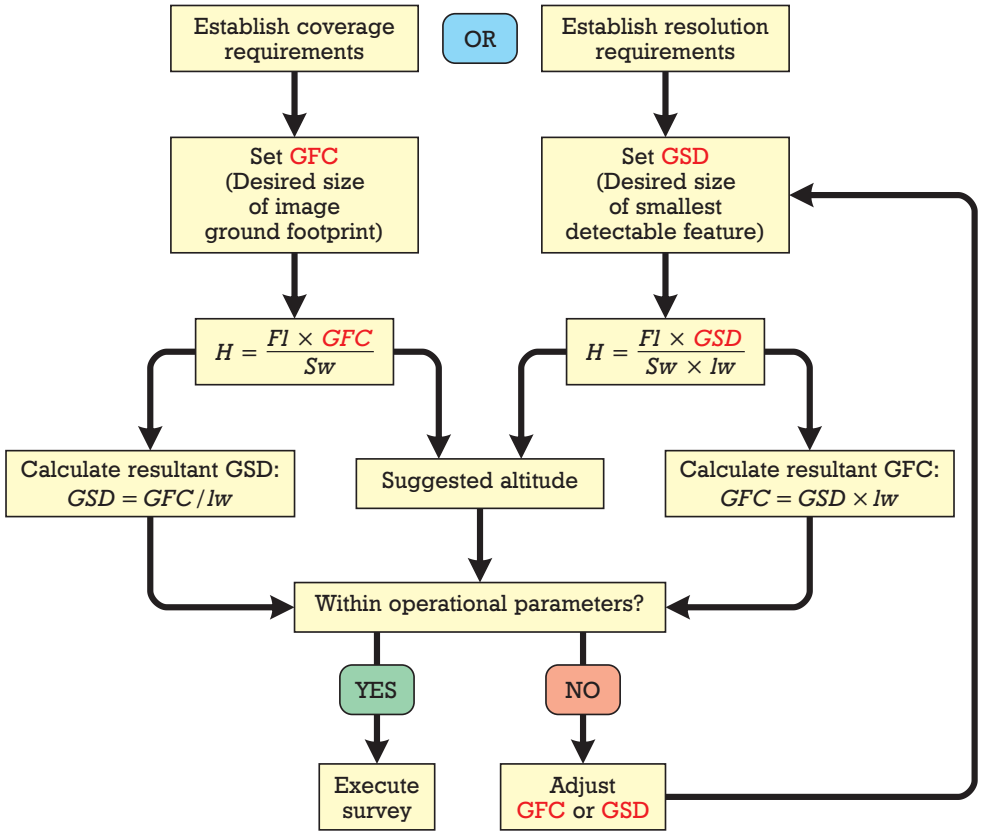

Figure 4: An example workflow for caclulating optimal survey altitude for a user defined GFC or GSD.

Figure 4 shows a suggested workflow for flight planning regarding controls for GFC and GSD using Equations 2 through 5. The initial step is to establish the operational requirements for coverage or resolution for the survey. Coverage requirements should be favoured if users are particularly constrained in terms of their data storage or processing power. Contrastingly, identification of resolution requirements should be of more concern to workers who wish to set specific limits for the scales of detectable features in their surveys. Once the user has established the required resolution and extent of their survey, they may choose a primary control variable (GSD or GFC) from which to begin the necessary calculations to find a suitable flying height. Desired values for image footprint extent or GSD may then be input to Equation 1 or 2 in order to calculate a suggested survey altitude. Users may also calculate the resultant counter-variable of their chosen control through employment of Equation 4 or 5. Once values for H, GFC and GSD have all been named or calculated, they must be checked to be within the operational parameters of the UAV platform, camera system, as well as the user's own abilities. For altitude, users must be responsible for not exceeding regulatory limits (Watts *et al.*, 2012). If calculated H, GFC or GSD are not within desirable limits, the surveyor may wish to adjust their quoted values for step 2 in order to improve coverage or resolution of their investigation. Once the user is satisfied that all parameters are within operational limits, the survey may be executed for the calculated altitude.

Limitations

The equations and protocols presented here, whilst easily applicable to a wide range of UAV imaging systems, cannot circumvent constraints of hardware limitations or altitude restrictions, however they are capable of aiding users in making the most of their available resources. Whilst GFC and GSD may be calculated as absolute values, the amount of error between the desired and actual values observed in survey outputs is dependent upon the accuracy of the UAV platform's altimeter or vertical autopilot (or the pilot's ability, if flying manually). Furthermore, GSD may not necessarily reflect the exact scale of distinguishable objects and is not a perfect proxy for resolution due to the effects of contrast and other variables. If users are concerned that landscape details or morphology of interest may not be detected in their survey because of this, slightly decreasing GSD beyond their desired value as a buffer may be advisable.

Conclusions

The ability for workers to identify the ideal survey altitude for their projects should not be understated, as it is the defining factor for the level of detail and volume of data captured during the survey. The use of UAVs for environmental surveying allows users to overcome the various difficulties and limitations of systems such as LiDAR or satellite-based sensing (Verstraete, 1996). Moreover, with adequate planning and implementation of the methods discussed in this paper, users are offered a good deal of flexibility (within their operational limits) to find an ideal compromise between survey resolution and data volume. Aftermarket software, often on a pay monthly basis, can assist with deployment of automated flights and are designed for speed and simplicity of operation. However, UAV surveying can often involve complex methods, intricate processing and bespoke mapping. The dynamic multiplicity of environments in which surveyors and researchers may find themselves operating can lead to variability in the challenges faced, and requirements for, gathering high quality data. As the field of environmental UAV surveying continues to develop, it is likely that different environments and survey subjects will develop specific methodologies suited to their particular traits and characteristics. Here this study acts as a strong foundation on which researchers and surveyors can base their own methodologies and tailored to circumvent challenges posed by their environment. By understanding the relationship between, altitude, coverage and resolution, the most important controls on the quality of survey output data, users can better plan around other factors such as the required battery and data storage capacities. Planning carried out well in advance of field operations will similarly allow workers to select (and if necessary, purchase) the most suitable hardware for their survey such as UAV platforms, cameras, or simply lenses. Overall, the protocols and workflows described in this paper are not a 'one-size-fits-all' solution; they provide a substantial base from which users can individually plan methodologies for the conditions of their project.

References

Colomina, I. & Molina, P. (2014). Unmanned aerial systems for photogrammetry and remote sensing: A review. *ISPRS Journal Of Photogrammetry And Remote Sensing*, 92, 79-97.

Commercial UAV Manufacturers. (2016). Uavglobal.com. Retrieved 24 May 2016, from http://www.uavglobal.com/commercial-uav-manufacturers/

Cunliffe, A., Brazier, R., & Anderson, K. (2016). Ultra-fine grain landscape-scale quantification of dryland vegetation structure with drone-acquired structure-from-motion photogrammetry. *Remote Sensing of Environment*, 183, 129-143.

Entwistle, N. S., & Heritage, G. L. (2019). Small unmanned aerial model accuracy for photogrammetrical fluvial bathymetric survey. *Journal of Applied Remote Sensing*, *13*(1), 014523.

Fonstad, M., Dietrich, J., Courville, B., Jensen, J., & Carbonneau, P. (2013). Topographic structure from motion: a new development in photogrammetric measurement. *Earth Surface Processes and Landforms*, 38(4), 421-430.

Goetz, A., Vane, G., Solomon, J., & Rock, B. (1985). *Imaging Spectrometry for Earth Remote Sensing*. *Science*, 228(4704), 1147-1153.

Goldhagen, P., Clem, J., & Wilson, J. (2003). Recent results from measurements of the energy spectrum of cosmic-ray induced neutrons aboard an ER-2 airplane and on the ground. *Advances In Space Research*, 32(1), 35-40.

Haralick, R., Shanmugam, K., & Dinstein, I. (1973). Textural Features for Image Classification. *IEEE Transactions On Systems, Man, And Cybernetics*, 3(6), 610-621. http://dx.doi.org/10.1109/tsmc.1973.4309314

Harwin, S. & Lucieer, A. (2012). Assessing the Accuracy of Georeferenced Point Clouds Produced via Multi-View Stereopsis from Unmanned Aerial Vehicle (UAV) Imagery. *Remote Sensing*, 4(12), 1573-1599. http://dx.doi.org/10.3390/rs4061573

Hodgson, A., Kelly, N., & Peel, D. (2013). Unmanned Aerial Vehicles (UAVs) for Surveying Marine Fauna: A Dugong Case Study. *Plos ONE*, 8(11), e79556.

McDonald, R. (1997). *Corona*. Bethesda, MD: American Society for Photogrammetry and Remote Sensing.

Moudrý, V., Gdulová, K., Fogl, M., Klápště, P., Urban, R., Komárek, J., Moudrá, L., Štroner, M., Barták, V. and Solský, M., 2019. Comparison of leaf-off and leaf-on combined UAV imagery and airborne LiDAR for assessment of a post-mining site terrain and vegetation structure: Prospects for monitoring hazards and restoration success. *Applied Geography*, 104, pp.32-41.

Moudrý, V., Gdulová, K., Fogl, M., Klápště, P., Urban, R., Komárek, J., Moudrá, L., Štroner, M., Barták, V. and Solský, M., (2019). Comparison of leaf-off and leaf-on combined UAV imagery and airborne LiDAR for assessment of a post-mining site terrain and vegetation structure: Prospects for monitoring hazards and restoration success. *Applied Geography*, 104, pp.32-41.

Neitzel, F. & Klonowski, J. (2012). Mobile 3d Mapping With A Low-Cost Uav System. *International Archives of the Photogrammetry, Remote Sensing and Spatial Information Sciences.*, XXXVIII-1/C22, 39-44.

Neugirg, F., Stark, M., Kaiser, A., Vlacilova, M., Della Seta, M., & Vergari, F. et al. (2016). Erosion processes in calanchi in the Upper Orcia Valley, Southern Tuscany, Italy based on multitemporal high-resolution terrestrial LiDAR and UAV surveys. *Geomorphology*, 269, 8-22.

Nex, F. & Remondino, F. (2013). UAV for 3D mapping applications: a review. *Applied Geomatics*, 6(1), 1-15.

Perry, R. (2012). *History of satellite reconnaissance.* Chantilly, VA: Center for the Study of National Reconnaissance.

Scott, S., Bui, T., Chan, K., & Bowen, S. (1990). The Meteorological Measurement System on the NASA ER-2 Aircraft. *Journal of Atmospheric and Oceanic Technology.* 7(4), 525-540.

Shahbazi, M., Sohn, G., Théau, J., & Menard, P. (2015). Development and Evaluation of a UAV-Photogrammetry System for Precise 3D Environmental Modeling. *Sensors*, 15(11), 27493-27524.

Siebert, S. & Teizer, J. (2014). Mobile 3D mapping for surveying earthwork projects using an Unmanned Aerial Vehicle (UAV) system. *Automation In Construction*, 41, 1-14.

THE DRONES REPORT: Market forecasts, a. (2016). THE DRONES REPORT: Market forecasts, regulatory barriers, top vendors, and leading commercial applications. Business Insider. Retrieved 24 May 2016, from http://uk.businessinsider.com/uav-or-commercial-drone-market-forecast-2015-2?r=US&IR=T

Turner, D., Lucieer, A., & Watson, C. (2012). An Automated Technique for Generating Georectified Mosaics from Ultra-High Resolution Unmanned Aerial Vehicle (UAV) Imagery, Based on Structure from Motion (SfM) Point Clouds. *Remote Sensing*, 4(12), 1392-1410.

Turner, I., Harley, M., & Drummond, C. (2016). UAVs for coastal surveying. Coastal Engineering, 114, 19-24.

Uysal, M., Toprak, A., & Polat, N. (2015). DEM generation with UAV Photogrammetry and accuracy analysis in Sahitler hill. *Measurement*, 73, 539-543.

Verstraete, M. (1996). Potential and limitations of information extraction on the terrestrial biosphere from satellite remote sensing. *Remote Sensing Of Environment*, 58(2), 201-214.

Watts, A., Ambrosia, V., & Hinkley, E. (2012). Unmanned Aircraft Systems in Remote Sensing and Scientific Research: Classification and Considerations of Use. *Remote Sensing*, 4(12), 1671-1692.